Bralower, T.J., Premoli Silva, I., and Malone, M.J. (Eds.)
Proceedings of the Ocean Drilling Program, Scientific Results Volume 198

13. Data Report: Geochemistry of Fine Fraction Carbonate Sediments, Shatsky Rise (ODP Leg 198)[1]

Mitchell J. Malone[2]

ABSTRACT

A detailed geochemical investigation was conducted of Upper Cretaceous to Holocene sediments recovered during Ocean Drilling Program (ODP) Leg 198 from Shatsky Rise, Pacific Ocean. The specific focus of this study was the geochemistry of 170 carbonate fine fraction samples from Sites 1207–1212. The geochemical data included in this report are carbonate content, stable carbon and oxygen isotope values, and elemental content (Ca, Mg, Sr, Ba, Fe, and Mn).

INTRODUCTION

Over the last several decades, a great deal of effort and progress has been made in reconstructing past ocean temperature and composition. Several approaches have been used ranging from elemental and isotopic composition of bulk carbonate sediments, marine cements, foraminiferal and other shells, pore fluids, and fluid inclusions (e.g., Renard, 1986; Wilson and Opdyke, 1996; Andreasson and Schmitz, 1998; Cicero and Lohmann, 2001; Lowenstein et al., 2001, Zachos et al., 2001). For parameters typically measured (e.g., $CaCO_3$, $\delta^{13}C$, $\delta^{18}O$, Sr, and $^{87}Sr/^{86}Sr$), the sources of secular variability are reasonably well understood, although more recent work has added complexity to our understanding of these processes (e.g., Stoll and Schrag, 1998; Martin et al., 1999; de Villiers, 1999). For many other elements, much less is understood about the controls on oceanic variability. The most common and successful techniques utilize carbonate sediments and shells; however, the fidelity

[1]Malone, M.J., 2005. Data report: geochemistry of fine fraction carbonate sediments, Shatsky Rise (ODP Leg 198). *In* Bralower, T.J., Premoli Silva, I., and Malone, M.J. (Eds.), *Proc. ODP, Sci. Results*, 198, 1–18 [Online]. Available from World Wide Web: <http://www-odp.tamu.edu/publications/198_SR/VOLUME/CHAPTERS/121.PDF>. [Cited YYYY-MM-DD]
[2]Integrated Ocean Drilling Program and Department of Geology and Geophysics, Texas A&M University, College Station TX 77845-9547, USA.
malone@iodp.tamu.edu

Initial receipt: 25 September 2004
Acceptance: 25 February 2005
Web publication: 7 July 2005
Ms 198SR-121

of the record is often limited by near-surface or burial diagenesis. Although much of past research has focused on isotopic records, a growing literature on elemental variation has led to a better understanding of variability of elements like Sr (e.g., Graham et al., 1982; Renard, 1986; Delaney and Boyle, 1988; Baker et al., 1990; Delaney and Linn, 1993; Hampt and Delaney, 1997; Andreasen and Delaney, 2000a). Despite the effort focused on Sr, as pointed out by Andreasen and Delaney (2000b), significant scatter and differences exist in these records. Although there are several possible explanations for such discrepancies (e.g., uncertainties in age, bulk, fine fraction, or individual component analysis), the real difficulty is diagenetic alteration of the primary signal and identification of the primary signal within the record.

Compared to other carbonate depositional environments, the diagenetic alteration of pelagic carbonates is generally well understood. The main driving forces for recrystallization are pressure solution (e.g., Schlanger and Douglas, 1974; Baker et al., 1980) and the excess free energy difference associated with small and delicate biogenic surfaces (e.g., Baker et al., 1982; Walter and Morse, 1984). A variety of models has been developed to better understand calcite recrystallization, most based on Sr exchange (e.g., Baker et al., 1982; Stout, 1985; Richter and De Paolo, 1987, 1988; Richter and Liang, 1993) and oxygen isotopes (e.g., Schrag et al., 1995) as diagenetic tracers. These all generally relate rates of recrystallization to depth and/or age, although the conclusions reached vary to some extent.

Delaney (1989) added to previous work by incorporating a model of temporal variation in interstitial water composition to more successfully predict observed calcite geochemistry. Moreover, she concluded that site-specific characteristics such as accumulation history, interstitial water chemistry, and its temporal variation must be taken into account to properly evaluate the effects of diagenesis. More recently, rather than making general uniform depth or age trend assumptions, studies have focused on detailed site-specific diagenetic complexities such as lithologic variability (e.g., Frank et al., 1999; Andreasen and Delaney, 2000b). The conclusions from these studies suggest that making uniform depth-age assumptions in pelagic carbonates is not universally applicable and may be an oversimplification.

During Leg 198, we obtained good-to-excellent recovery of Neogene through Upper Cretaceous pelagic sediments (Bralower, Premoli Silva, Malone, et al., 2002). Based on visual observation, physical property data (Eocene-Cretaceous underconsolidation), and interstitial water geochemistry, Leg 198 sediments are undergoing recrystallization but at apparently very low rates. The transition from ooze to chalk is not observed in Upper Cretaceous and younger sediments. In fact, the very low rates determined by Richter and Liang (1993) at Deep Sea Drilling Project (DSDP) Site 305 located on the Southern High at Shatsky Rise were so different from other deep-sea sites that they invoked downhole contamination of pore waters during rotary drilling to explain the abnormally low recrystallization rate. We recored Site 305 during Leg 198 (Site 1211) with the advanced piston corer (APC), and the interstitial water Sr profiles are very similar. Hence, downhole contamination cannot explain the very low estimated recrystallization rates. However, using the same Sr/Ca ratios from pore waters at Site 305 and bulk carbonate Sr/Ca ratios reported in Matter et al. (1975), Baker et al. (1982) concluded that 50% of the carbonate had recrystallized by 100 meters below seafloor (mbsf), 75% at 200 mbsf, and 95% by 500 mbsf. Clearly, different diagenetic models using similar data sets produced

different results, and a more detailed investigation is required to explain these discrepancies. Leg 198 sediments provide an opportunity to determine the degree of recrystallization of Shatsky Rise sediments, to assess the fidelity of the primary record, and to test fundamental assumptions with pelagic carbonate diagenetic models. This data report provides the initial data set for future work.

METHODS

For this report, 170 samples were collected at a frequency of one per core at each site and analyzed as described below. We chose to focus on just the fine fraction for this study for the following reasons. The dominant carbonate pelagic component in Shatsky Rise sediments is not consistent throughout the studied interval. Neogene sediments are dominated by nannofossils, whereas Paleogene and Upper Cretaceous sediments are dominated by foraminifers (Bralower, Premoli Silva, Malone, et al., 2002). In general, foraminifers and nannofossils are inferred to have different elemental partition coefficients and, thus, incorporate minor and trace elements at different levels (e.g., Elderfield et al., 1982; Delaney et al., 1985; Stout, 1985; Andreasen and Delaney, 2000a; Stoll et al., 2002). Fine fraction has been preferred over bulk sediments for elemental secular variability studies (e.g., Baker et al., 1990; Andreasen and Delaney, 2000a). Therefore, to avoid changes in sediment components obscuring diagenetic or secular trends, the fine fraction was the focus of the present study.

Approximately 1 g of sediment was immersed in Chlorox at 60°C to oxidize organic matter and disaggregate sediment particles. Chlorox was chosen for this step because it has been shown to effectively remove organics without dissolving calcium carbonate (Gaffey and Bronnimann, 1993; Pingitore et al., 1993). The resulting slurry was passed through a 63-µm sieve and the fine fraction retained, rinsed, and dried. A split of each fine fraction sample was retained for carbonate and stable isotopic analyses.

Each fine fraction split was analyzed for stable oxygen and carbon isotopic ratios. Approximately 120 µg of powdered sample was reacted in "100%" phosphoric acid at 70°C in an online, automated Kiel device coupled to a Finnigan MAT 251 stable isotope ratio mass spectrometer. The carbonate standard NBS-19 ($\delta^{13}C$ = 1.95‰; $\delta^{18}O$ = –2.20‰) was used to calibrate to the Vienna Peedee belemnite (VPDB) standard. Repeated analyses of NBS-19 yielded reproducibility of 0.08‰ for $\delta^{18}O$ and 0.04‰ for $\delta^{13}C$.

Calcium carbonate content was determined on ~10 mg of each fine fraction split using a UIC, Inc., Coulometrics model 5011 CO_2 coulometer. Average relative standard deviation from the mean of replicate samples is better than 1 wt% $CaCO_3$.

Fine fraction sediments were treated with a cleaning protocol similar to that of Andreasen and Delaney (2000b), which was a modification of the method developed by Aptiz (1991), to ensure that the elemental data measured were from calcite alone. Approximately 30 mg of carbonate-rich samples (>65 wt% $CaCO_3$) or ~50 mg of carbonate-poor samples (<65 wt%) was precisely weighed and placed in 50 mL acid-cleaned, polypropylene centrifuge tubes to reduce oxyhydroxides and remove exchangeable ions. First, 10 mL of reducing solution (25 g $NH_2OH{\cdot}HCl$ + 200 mL 14.5-M NH_4OH + 300 mL nanopure water) was

added and shaken at room temperature overnight, and then centrifuged. The solution was discarded and the reducing procedure repeated. Next, 10 mL of ion exchange solution (1-M NH_4OH) was added, shaken for 1 hr, centrifuged, and the solution discarded. The sample was dried and then dissolved for 1.5 hr in 1-M acetic acid solution buffered with 1-M ammonium acetate (pH = 5) on a shaker table at room temperature. A 2-mL aliquot of this solution was removed with a volumetric pipette, dispensed into acid-cleaned high-density polyethylene bottles, and diluted with 10 mL of 1-N trace metal grade nitric acid for analyses.

Solutions were analyzed for Ca, Mg, Sr, Fe, Mn, and Ba on a Spectro CirOS inductively coupled plasma-optical emission spectrometer (ICP-OES). Precision of analyses (relative standard deviation from the mean) determined by replicate analyses of internal standards and samples was as follows: Ca = 1.7%, Mg = 2.5%, Sr = 1.3%, Mn = 2.3%, and Ba = 7%. Sample replicates show generally poor reproducibility for Fe: mean = 28%. The poorest results are associated with samples low in Fe (<200 ppm). A replicate with high Fe content (~1500 ppm) resulted in relatively good precision of 4%. It is not clear if poor Fe reproducibility is the result of ineffective removal of noncarbonate Fe (e.g., oxyhydroxides), low concentrations, or some other factor that remains to be identified. Note, however, that Mn, also a common contaminant in oxyhydroxides, shows good reproducibility, including low content replicants (~13 ppm). Fe data are listed for completeness, but these data should be treated with caution. Minor elements are reported as parts per million in total carbonate. As reported previously, calcium self-absorption in the ICP plasma results in curvature of sensitivity at high concentrations (i.e., a matrix effect) (e.g., Rosenthal et al., 1999; de Villiers et al., 2002). Such a Ca matrix effect was noted for samples with $CaCO_3$ higher than ~90 wt%. Therefore, minor element parts per million in total carbonate was calculated using $CaCO_3$ determined from coulometric analyses rather than calculated from Ca analyses.

RESULTS

Fine fraction geochemical data are compiled in Table **T1** and are shown graphically in Figures **F1**, **F2**, **F3**, **F4**, **F5**, **F6**, and **F7**. Although none of the samples were selected following the stratigraphic splice, figures show data plotted vs. meters composite depth (mcd) for easier comparison to other studies, except at Sites 1207 and 1208 where composite sections were not possible. Figure **F6** shows Sr and Mg content from this study and from DSDP Site 305 (reoccupied at Site 1211) reported in Matter et al. (1975). Although Site 305 data are from bulk and not fine fraction analyses, the trends and absolute values compare well.

All sites show the same general trend in carbonate content, varying between 33 wt% and almost pure carbonate (99.8 wt%). Neogene and Paleogene sediments are characterized by variable carbonate content, whereas Cretaceous sediments are uniform and very carbonate-rich (>90 wt%).

At all sites, $\delta^{18}O$ decreases with depth, ranging from 2.1‰ to –1.7‰, with the most negative values in Cretaceous sediments. The sharpest decreases in $\delta^{18}O$ are found at Sites 1207 and 1208, where little to no Paleogene sediment was recovered. The sites on the Southern High (Sites 1209–1212) show more gradual $\delta^{18}O$ decreases through the Neogene and Paleogene sections. At Site 1211, $\delta^{18}O$ values increase below

T1. Carbonate geochemistry, p. 15.

F1. Geochemical data vs. depth, Site 1207, p. 8.

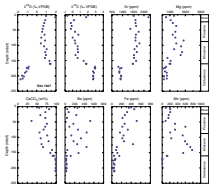

F2. Geochemical data vs. depth, Site 1208, p. 9.

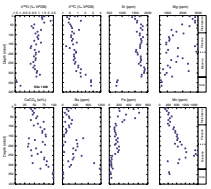

F3. Geochemical data vs. depth, Site 1209, p. 10.

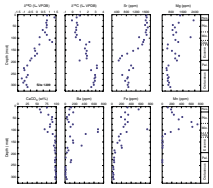

F4. Geochemical data vs. depth, Site 1210, p. 11.

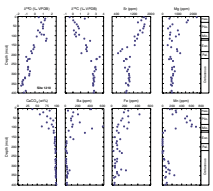

F5. Geochemical data vs. depth, Site 1211, p. 12.

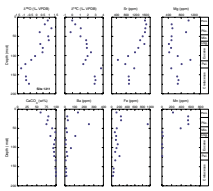

the $\delta^{18}O$ minimum in the uppermost Cretaceous, although values remain negative.

In contrast to the $\delta^{18}O$ trend, $\delta^{13}C$ values generally increase with depth, ranging from –0.7‰ to 3.3‰, although the increase is mostly apparent in Neogene and Paleogene sediments. $\delta^{13}C$ values within Cretaceous sediments are uniform compared to younger sediments.

Sr content varies from 460 to 2211 ppm. At Sites 1207 and 1208, the Sr trend mirrors $\delta^{18}O$, sharply decreasing downhole at the transition into Cretaceous sediments. At the Southern High sites, Sr decreases downcore from maximum values at the top of the section to minimum values in the Eocene. Below the Eocene, Sr increases abruptly to values ~800–900 ppm, remaining uniform downcore.

Mg content ranges from 346 to 4011 ppm with highest values found in Pleistocene sediments. No clear consistent downcore trends in the Mg content are observed; however, a downcore Mg maxima is found in Eocene sediment at the Southern High sites that coincides with the Sr minimum, which is most pronounced at Site 1211 (Figs. F5, F6).

Ba contents (4–1161 ppm) are highly variable and elevated in the Neogene and Paleogene relative to the Cretaceous, where Ba is uniform and very low. The highest Ba contents are found in Miocene sediments at Sites 1207, 1209, and 1210.

Fe contents range from below the detection limit to 935 ppm. With the analytical uncertainty previously described, confidently identifying trends is not possible.

Mn concentrations in the fine fraction vary from below the detection limit to 1685 ppm. All sites show the same trend of increasing values downcore to a maximum peak in the Miocene then decreasing downcore to very low values in the Cretaceous.

ACKNOWLEDGMENTS

This research used samples and/or data provided by the Ocean Drilling Program (ODP). ODP is sponsored by the U.S. National Science Foundation (NSF) and participating countries under management of Joint Oceanographic Institutions (JOI), Inc. Funding for this research was provided by a NSF/JOI/U.S. Science Support Program (USSSP) grant. Stable isotopic analyses were performed in the Department of Geology and Geophysics, Texas A&M University (College Station, Texas, USA), under the direction of Dr. Ethan Grossman. Elemental analyses were performed by Bryan Brattin at the Trace Element Research Laboratory, Texas A&M University. Erin Lyons, Chris Yarborough, and Kristin Lehnhoff performed the sample processing, and I am indebted to their effort.

F6. Sr/Mg data vs. depth, Site 1211, p. 13.

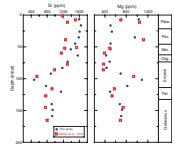

F7. Geochemical data vs. depth, Site 1212, p. 14.

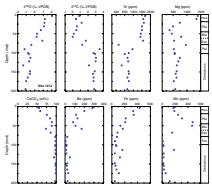

REFERENCES

Andreasen, G.H., and Delaney, M.L., 2000a. Bulk calcite size fraction distribution and Sr/Ca composition for deep-sea sediments at selected age horizons. *Mar. Geol.,* 169:185–205.

Andreasen, G.H., and Delaney, M.L., 2000b. Lithologic controls on calcite recrystallization in Cenozoic deep-sea sediments. *Mar. Geol.,* 163:109–124.

Andreasson, F.P., and Schmitz, B., 1998. Tropical Atlantic seasonal dynamics in the early middle Eocene from stable oxygen and carbon isotope profiles of mollusk shells. *Paleoceanography,* 13:183–192.

Aptiz, S.E., 1991. The Lithification of Ridge Flank Basal Carbonates: Characterization and Implications for Strontium/Calcium and Magnesium/Calcium in Marine Chalks. University of California, San Diego 304 p.

Baker, P.A., Gieskes, J.M., and Elderfield, H., 1982. Diagenesis of carbonates in deep-sea sediments—evidence from Sr^{2+}/Ca^{2+} ratios and interstitial dissolved Sr^{2+} data. *J. Sediment. Petrol.,* 52:71–82.

Baker, P.A., Kastner, M., Byerlee, J.D., and Lockner, D.A., 1980. Pressure solution and hydrothermal recrystallization of carbonate sediments—an experimental study. *Mar. Geol.,* 38:185–203.

Baker, P.A., Malone, M.J., Burns, S.J., and Swart, P.K., 1990. Minor element and stable isotopic composition of the carbonate fine fraction: Site 709, Indian Ocean. *In* Duncan, R.A., Backman, J., Peterson, L.C., et al., *Proc. ODP, Sci. Results,* 115: College Station, TX (Ocean Drilling Program), 661–675.

Bralower, T.J., Premoli Silva, I., Malone, M.J., et al., 2002. *Proc. ODP, Init. Repts.,* 198 [CD-ROM]. Available from: Ocean Drilling Program, Texas A&M University, College Station TX 77845-9547, USA.

Cicero, A., and Lohmann, K.C., 2001. Sr/Mg variation during rock-water interaction: implications for secular changes in the elemental chemistry of ancient seawater. *Geochim. Cosmochim. Acta,* 65:741–761.

Delaney, M.L., 1989. Temporal changes in interstitial water chemistry and calcite recrystallization in marine sediments. *Earth Planet. Sci. Lett.* 95:23–37.

Delaney, M.L., Bé, A.W.H., and Boyle, E.A., 1985. Li, Sr, Mg, and Na in foraminiferal calcite shells from laboratory culture, sediment traps, and sediment cores. *Geochim. Cosmochim. Acta,* 49:1327–1341.

Delaney, M.L., and Boyle, E.A., 1988. Tertiary paleoceanic chemical variability: unintended consequences of simple geochemical models. *Paleoceanography,* 3:137–156.

Delaney, M.L., and Linn, L.J., 1993. Interstitial water and bulk calcite chemistry, Leg 130, and calcite recrystallization. *In* Berger, W.H., Kroenke, L.W., Mayer, L.A., et al., *Proc. ODP, Sci. Results,* 130: College Station, TX (Ocean Drilling Program), 561–572.

de Villiers, S., 1999. Seawater strontium and Sr/Ca variability in the Atlantic and Pacific oceans. *Earth Planet. Sci. Lett.,* 171:623–634.

de Villiers, S., Greaves, M., and Elderfield, H., 2002. An intensity ratio calibration method for the accurate determination of Mg/Ca and Sr/Ca of marine carbonates by ICP-AES. *Geochem. Geophys. Geosys.,* 3:2001GC000169.

Elderfield, H., Gieskes, J., Baker, P.A., Oldfield, R.K., Hawkesworth, C.J., and Miller, R.J., 1982. $^{87}Sr/^{86}Sr$ and $^{18}O/^{16}O$ ratios, interstitial water chemistry and diagenesis in deep-sea carbonate sediments of the Ontong Java Plateau. *Geochim. Cosmochim. Acta*, 46:2259–2268.

Frank, T.D., Arthur, M.A., and Dean, W.E., 1999. Diagenesis of Lower Cretaceous pelagic carbonates, North Atlantic: paleoceanographic signals obscured. *J. Foram. Res.,* 29:340–351.

Gaffey, S.J., and Bronnimann, C.E., 1993. Effects of bleaching on organic and mineral phases in biogenic carbonates. *J. Sed. Petrol.,* 63:752–754.

Graham, D.W., Bender, M.L., Williams, D.F., and Keigwin, L.D., Jr., 1982. Strontium-calcium ratios in Cenozoic planktonic foraminifera. *Geochim. Cosmochim. Acta,* 46:1281–1292.

Hampt, G., and Delaney, M.L., 1997. Influences on calcite Sr/Ca records from Ceara Rise and other regions: distinguishing ocean history and calcite recrystallization. *In* Shackleton, N.J., Curry, W.B., Richter, C., and Bralower, T.J. (Eds.), *Proc. ODP, Sci. Results,* 154: College Station, TX (Ocean Drilling Program), 491–500.

Lowenstein, T.K., Timofeeff, M.N., Brennan, S.T., Hardie, L.A., and Demicco, R.V., 2001. Oscillations in Phanerozoic seawater chemistry: evidence from fluid inclusions. *Science,* 294:1086–1088.

Martin, P.A., Lea, D.W., Mashiotta, T.A., Papenfuss, T., and Sarnthein, M., 1999. Variation of foraminiferal Sr/Ca over Quaternary glacial-interglacial cycles: evidence for changes in mean ocean Sr/Ca? *Geochem. Geophys. Geosyst.,* 1:1999GC000006.

Matter, A., Douglas, R.G., and Perch-Nielsen, K., 1975. Fossil preservation, geochemistry and diagenesis of pelagic carbonates from the Shatsky Rise, northwest Pacific. *In* Larson, R.L., Moberly, R., et al., *Init. Repts. DSDP,* 32: Washington (U.S. Govt. Printing Office), 891–921.

Pingitore, N.E., Fretzdorf, S.B., et al., 1993. Dissolution kinetics of $CaCO_3$ in common laboratory solvents. *J. Sed. Petrol.,* 63:641–645.

Renard, M., 1986. Pelagic carbonate chemostratigraphy (Sr, Mg, ^{18}O, ^{13}C). *Mar. Micropaleontol.* 10:117–164.

Richter, F.M., and DePaolo, D.J., 1987. Numerical models of diagenesis and the Neogene Sr isotopic evolution of seawater from DSDP Site 590B. *Earth Planet. Sci. Lett.,* 83:27–38.

Richter, F.M., and DePaolo, D.J., 1988. Diagenesis and Sr isotopic evolution of seawater using data from DSDP 590B and 575. *Earth Planet. Sci. Lett.,* 90:382–394.

Richter, F.M., and Liang, Y., 1993. The rate and consequences of Sr diagenesis in deep-sea carbonates. *Earth Planet. Sci. Lett.,* 117:553–565.

Rosenthal, Y.M., Field, F., and Sherrell, R.M., 1999. Precise determination of element/calcium ratios in calcareous samples using sector field inductively coupled plasma mass spectrometry. *Anal. Chem.,* 71:3248–3253.

Schlanger, S.O., and Douglas, R.G., 1974. The pelagic ooze-chalk-limestone transition and its implication for marine stratigraphy. *In* Hsü, K.J., and Jenkyns, H.C. (Eds.), *Pelagic Sediments: On Land and Under the Sea.* Spec. Publ.—Int. Assoc. Sedimentol., 1:117–148.

Schrag, D.P., DePaolo, D.J., and Richter, F.M., 1995. Reconstructing past sea surface temperatures: correcting for diagenesis of bulk marine carbonate. *Geochim. Cosmochim. Acta,* 59:2265–2278.

Stoll, H.M., and Schrag, D.P., 1998. Effects of Quaternary sea level cycles on strontium in seawater. *Geochim. Cosmochim. Acta,* 62:1107–1118.

Stoll, H.M., Klaas, C., Probert, I.P., Ruiz-Encinar, J., and Garcia-Alonso, J.I., 2002. Calcification rate and temperature effects on Sr partitioning in coccoliths of multiple species of coccolithophorids. *Global Planet. Change*, 34:153–171.

Stout, P.M., 1985. Interstitial water chemistry and diagenesis of biogenic sediments from the eastern equatorial Pacific, Deep Sea Drilling Project Leg 85. *In* Mayer, L., Theyer, F., Thomas, E., et al., *Init. Repts. DSDP,* 85: Washington (U.S. Govt. Printing Office), 805–820.

Walter, L.M., and Morse, J.M., 1984. Reactive surface area of skeletal carbonates during dissolution: effect of grain size. *J. Sed. Petrol.,* 54:1081–1090.

Wilson, P.A., and Opdyke, B.N., 1996. Equatorial sea-surface temperatures for the Maastrichtian revealed through remarkable preservation of metastable carbonate. *Geology,* 24:555–558.

Zachos, J.C., Pagani, M., Sloan, L., Thomas, E., and Billups, K., 2001. Trends, rhythms, and aberrations in global climate 65 Ma to present. *Science,* 292:686–693.

Figure F1. Site 1207 fine fraction geochemical data vs. depth. VPDB = Vienna Peedee belemnite.

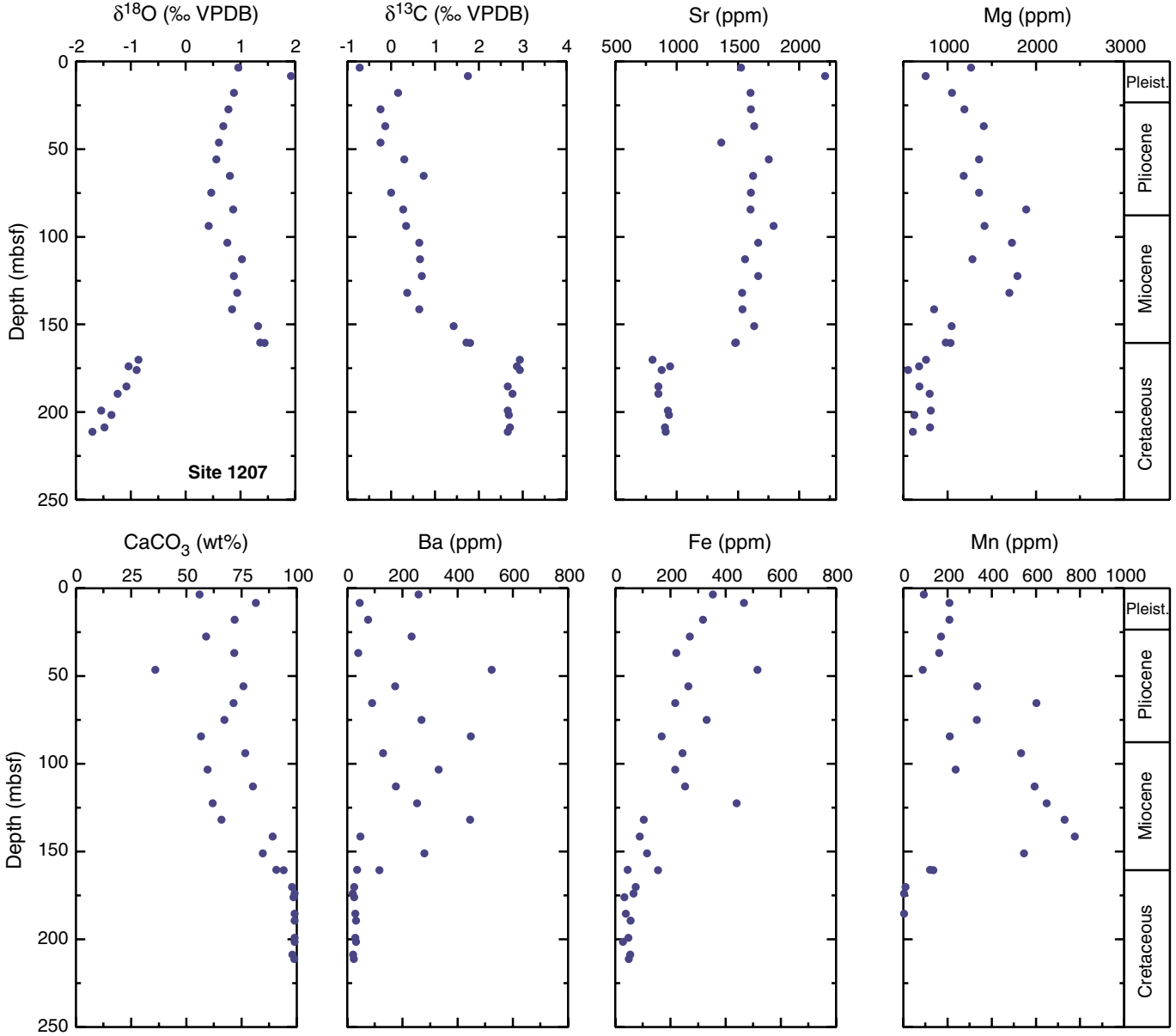

Figure F2. Site 1208 fine fraction geochemical data vs. depth. VPDB = Vienna Peedee belemnite.

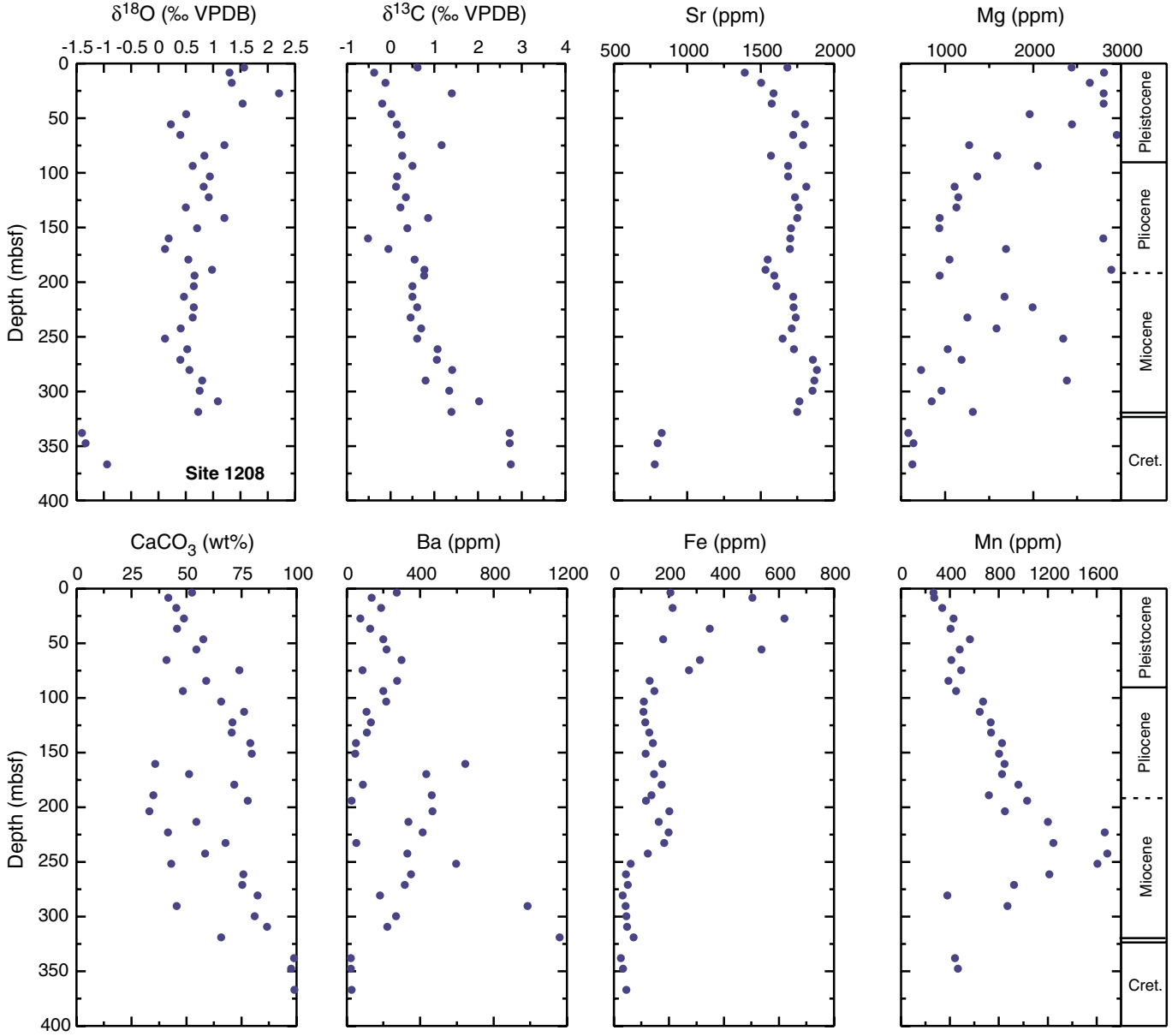

Figure F3. Site 1209 fine fraction geochemical data vs. depth. VPDB = Vienna Peedee belemnite.

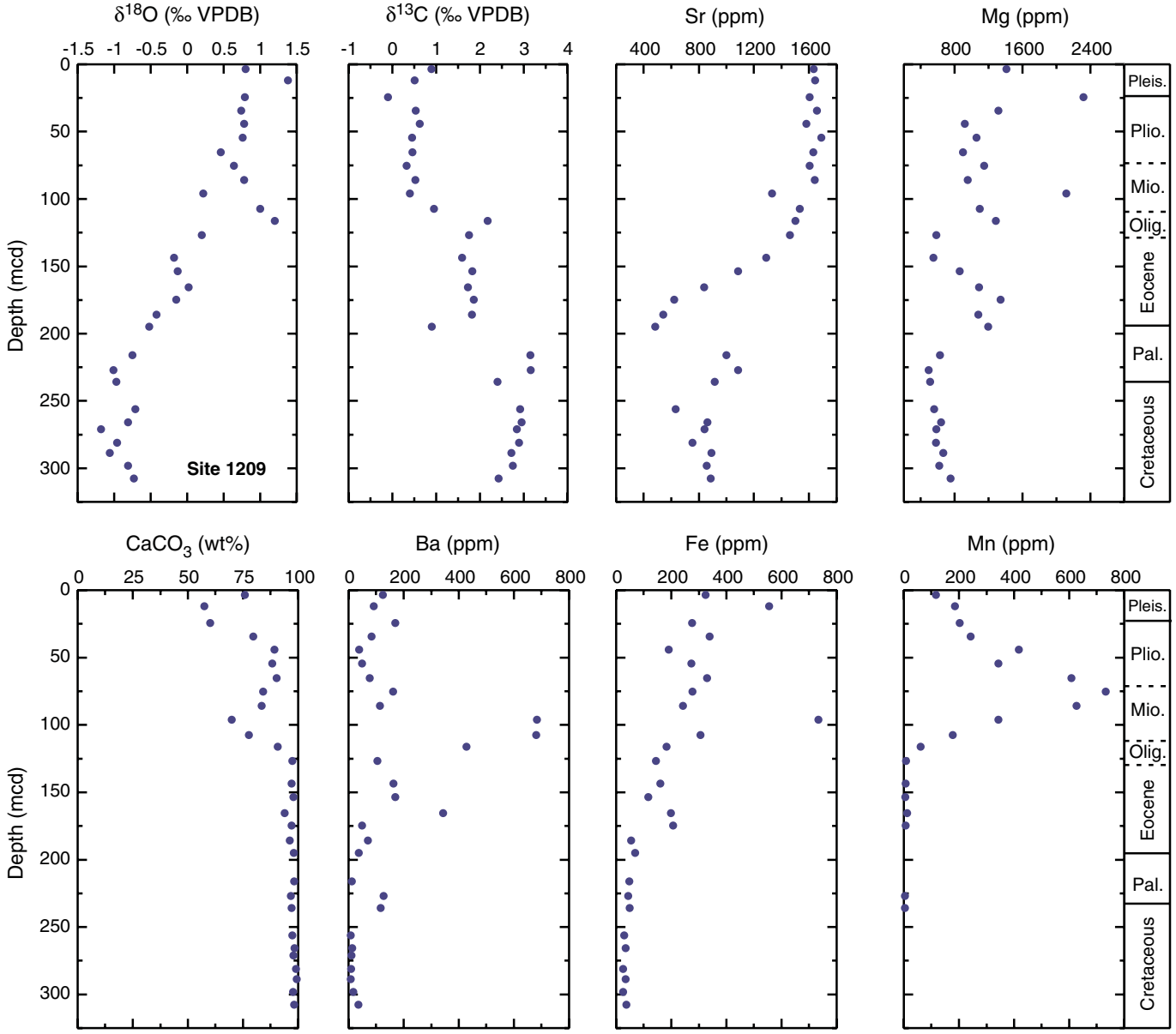

Figure F4. Site 1210 fine fraction geochemical data vs. depth. VPDB = Vienna Peedee belemnite.

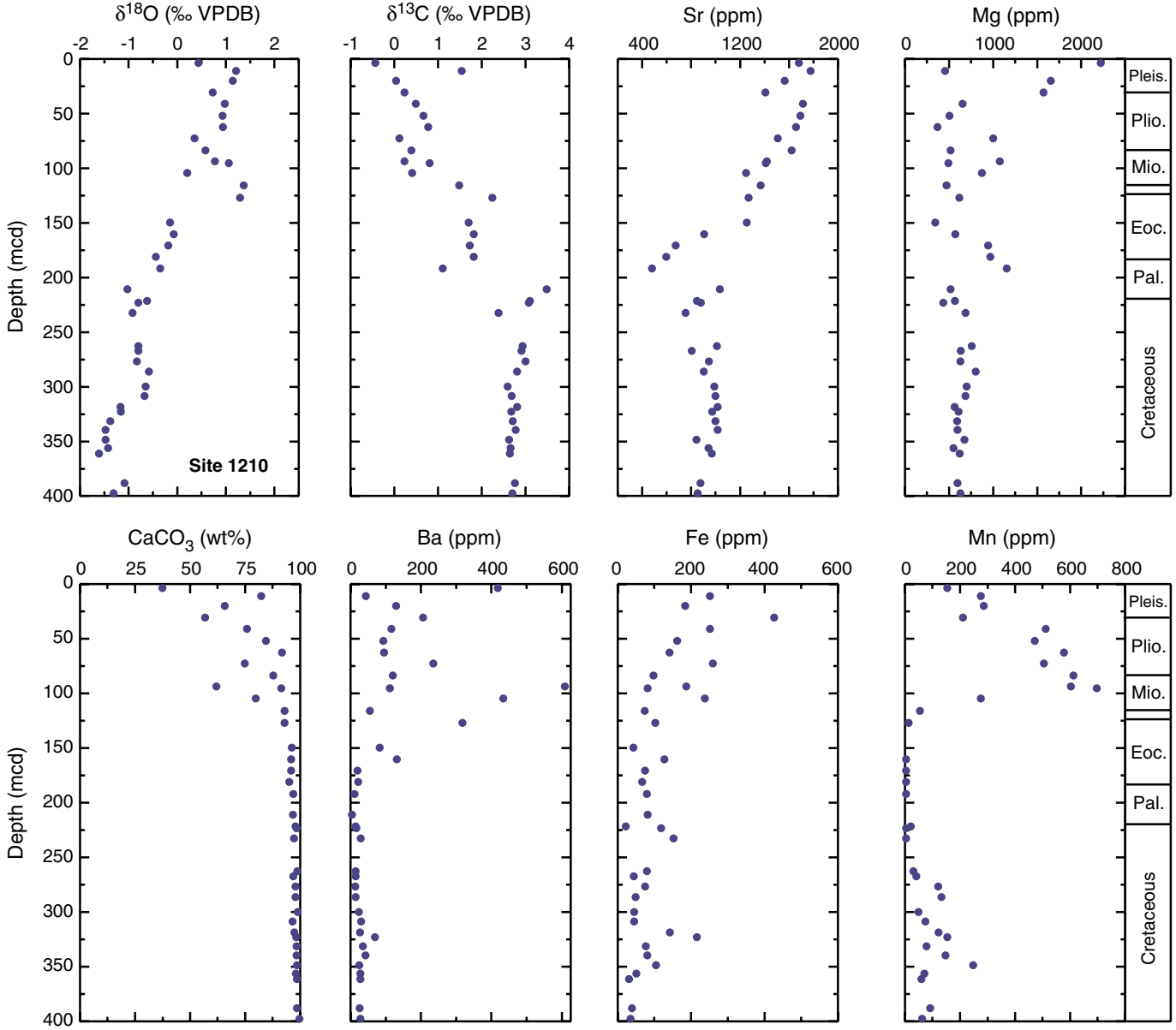

Figure F5. Site 1211 fine fraction geochemical data vs. depth. VPDB = Vienna Peedee belemnite.

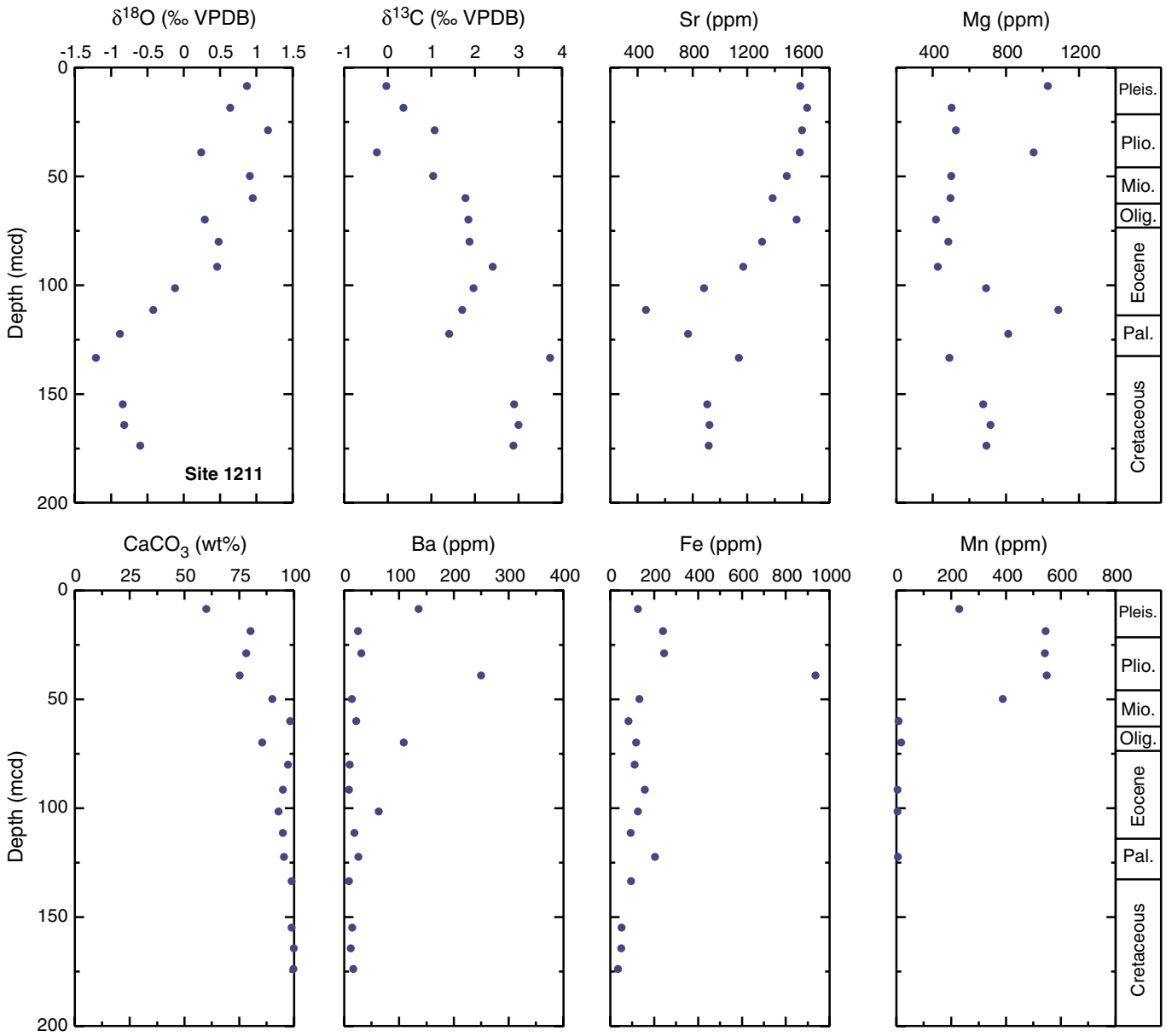

Figure F6. Site 1211 fine fraction Sr and Mg plotted with bulk carbonate data from Matter et al., 1975, Site 305.

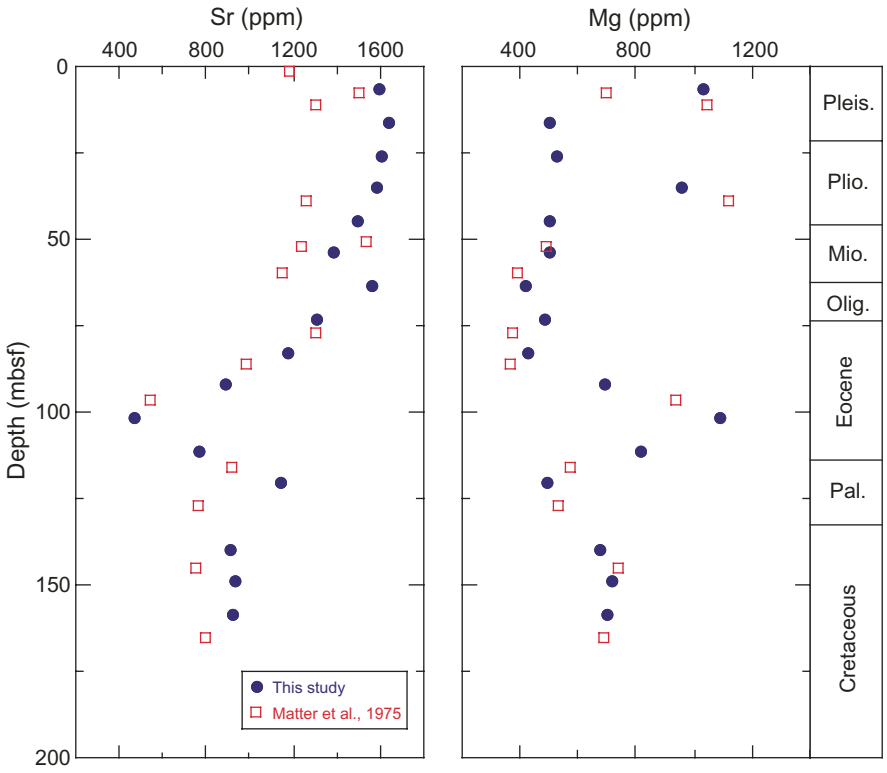

Figure F7. Site 1212 fine fraction geochemical data vs. depth. VPDB = Vienna Peedee belemnite.

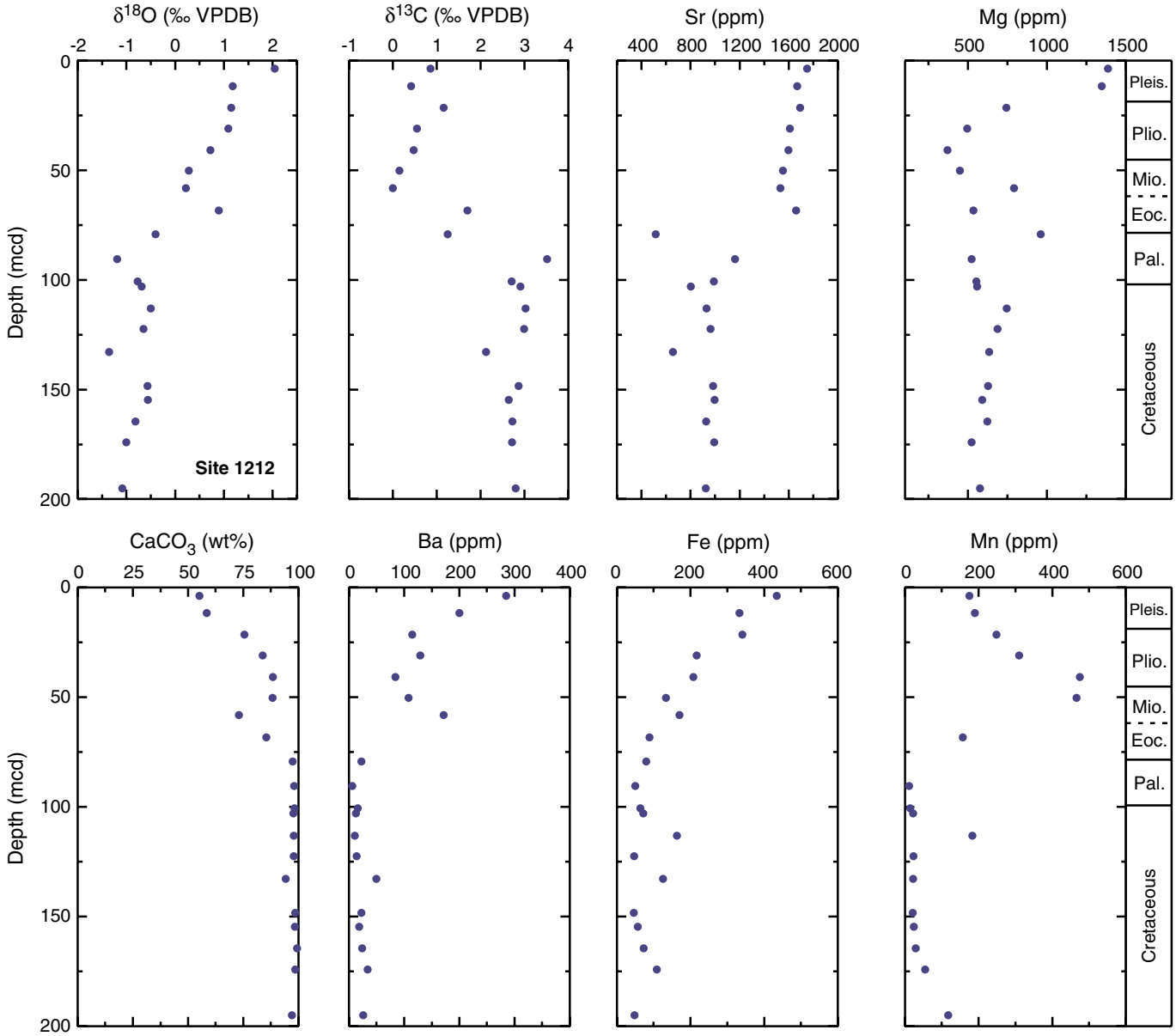

Table T1. Geochemistry of carbonate fine fraction. (See table note. Continued on next two pages.)

Core, section, interval (cm)	Depth (mbsf)	Fine iso	Depth (mcd)	Stable isotopes (% VPDB)		$CaCO_3$ (wt%)	Minor elements (ppm)				
				$\delta^{13}C$	$\delta^{18}O$		Sr	Mg	Ba	Fe	Mn
198-1207A-											
1H-3, 60–62	3.60	SR293	3.60	0.71	0.96	56.0	1525	1266	259	354	93
2H-3, 60–62	8.40	SR294	8.40	1.75	1.92	81.4	2211	752	46	466	209
3H-3, 60–62	17.90	SR295	17.90	0.16	0.88	71.8	1602	1052	76	318	209
4H-3, 60–62	27.40	SR296	27.40	0.24	0.78	58.9	1606	1190	233	270	171
5H-3, 60–62	36.90	SR297	36.90	0.13	0.69	71.6	1634	1411	40	221	163
6H-3, 58–60	46.38	SR298	46.38	0.24	0.61	35.9	1365	4011	524	515	89
7H-3, 60–62	55.90	SR299	55.90	0.30	0.56	75.9	1752	1357	174	265	335
8H-3, 60–62	65.40	SR300	65.40	0.74	0.81	71.4	1625	1182	90	217	602
9H-3, 60–62	74.90	SR301	74.90	0.00	0.47	67.3	1605	1357	269	331	333
10H-3, 60–62	84.40	SR302	84.40	0.28	0.87	56.6	1604	1890	447	168	210
11H-3, 60–62	93.90	SR303	93.90	0.34	0.42	76.7	1791	1419	130	244	533
12H-3, 60–62	103.40	SR304	103.40	0.64	0.76	59.6	1666	1728	331	218	237
13H-3, 60–62	112.90	SR305	112.90	0.66	1.03	80.2	1559	1284	177	253	595
14H-3, 60–62	122.40	SR306	122.40	0.70	0.88	62.0	1664	1790	253	440	650
15H-3, 60–62	131.90	SR307	131.90	0.37	0.94	65.9	1533	1700	445	103	730
16H-3, 60–62	141.40	SR308	141.40	0.64	0.85	89.1	1538	847	48	89	777
17H-3, 60–62	150.90	SR309	150.90	1.43	1.32	84.6	1631	1046	279	115	547
18H-3, 60–62	160.40	SR310	160.40	1.72	1.36	90.7	1485	979	36	46	121
20H-3, 60–62	175.90	SR311	175.90	2.93	–0.89	98.5	878	554	25	33	BDL
21X-3, 60–62	185.40	SR312	185.40	2.66	–1.08	99.0	853	684	30	39	4
23X-3, 60–62	201.50	SR313	201.50	2.69	–1.35	99.1	939	625	32	28	BDL
24X-3, 60–62	211.20	SR314	211.20	2.66	–1.70	98.9	913	607	24	49	BDL
198-1207B-											
1R-3, 60–62	160.60	SR315	160.60	1.80	1.44	94.1	1477	1036	116	155	136
2R-3, 60–62	170.20	SR316	170.20	2.93	–0.86	97.8	804	758	26	75	10
2R-5, 138–140	173.98	SR317	173.98	2.87	–1.04	99.1	946	679	20	67	4
4R-3, 60–62	189.40	SR318	189.40	2.77	–1.24	99.1	852	799	32	56	BDL
5R-3, 60–62	199.10	SR319	199.10	2.66	–1.54	99.0	928	809	30	48	BDL
6R-3, 60–62	208.70	SR320	208.70	2.71	–1.48	98.1	905	804	22	55	BDL
198-1208A-											
1H-3, 60–62	3.60	SR321	3.60	0.62	1.57	52.5	1682	2438	272	206	267
2H-3, 60–62	8.30	SR322	8.30	0.37	1.30	41.7	1391	2806	136	504	273
3H-3, 60–62	17.80	SR323	17.80	0.11	1.34	45.4	1504	2643	188	213	337
4H-3, 60–62	27.30	SR324	27.30	1.40	2.21	48.9	1589	2802	73	620	431
5H-3, 60–62	36.80	SR325	36.80	0.19	1.54	45.7	1575	2801	128	348	407
6H-3, 60–62	46.30	SR326	46.30	0.02	0.51	57.6	1736	1962	200	179	564
7H-3, 60–62	55.80	SR327	55.80	0.14	0.23	54.5	1802	2440	217	536	481
8H-3, 60–62	65.30	SR328	65.30	0.25	0.40	41.0	1722	2951	298	312	412
9H-3, 60–62	74.80	SR329	74.80	1.17	1.21	74.1	1790	1275	86	273	491
10H-3, 60–62	84.30	SR330	84.30	0.27	0.84	59.0	1571	1592	275	130	388
11H-3, 60–62	93.80	SR331	93.80	0.50	0.63	48.3	1687	2052	198	147	451
12H-3, 60–62	103.30	SR332	103.30	0.15	0.94	65.8	1687	1366	214	109	672
13H-3, 60–62	112.80	SR333	112.80	0.13	0.83	76.2	1811	1110	107	108	643
14H-3, 60–62	122.30	SR334	122.30	0.35	0.92	70.9	1735	1150	132	114	733
15H-3, 60–62	131.80	SR335	131.80	0.23	0.50	70.5	1759	1128	110	129	736
16H-3, 60–62	141.30	SR336	141.30	0.86	1.21	78.9	1749	938	50	142	826
17H-3, 60–62	150.80	SR337	150.80	0.38	0.71	79.7	1706	934	46	115	801
18H-3, 60–62	160.30	SR338	160.30	0.52	0.19	35.7	1703	2798	647	176	846
19H-3, 60–62	169.80	SR339	169.80	0.05	0.12	51.2	1699	1691	434	146	826
20H-3, 60–62	179.30	SR340	179.30	0.55	0.55	71.7	1548	1050	87	174	960
21X-3, 60–62	188.80	SR341	188.80	0.78	0.98	35.0	1534	2886	463	137	717
22X-3, 60–62	194.00	SR342	194.00	0.77	0.66	77.9	1592	940	25	117	1032
23X-3, 60–62	203.70	SR343	203.70	0.50	0.65	33.2	1608	3009	467	201	849
24X-3, 60–62	213.40	SR344	213.40	0.50	0.47	54.5	1723	1675	336	163	1200
25X-3, 60–62	223.00	SR345	223.00	0.61	0.65	41.6	1724	1993	413	199	1666
26X-3, 60–62	232.70	SR346	232.70	0.46	0.63	67.8	1740	1255	52	183	1245
27X-3, 60–62	242.30	SR347	242.30	0.70	0.41	58.4	1712	1584	330	123	1685
28X-3, 60–62	251.70	SR348	251.70	0.61	0.12	43.1	1650	2343	596	61	1608
29X-3, 60–62	261.40	SR349	261.40	1.08	0.53	75.9	1726	1030	350	44	1213
30X-3, 60–62	271.00	SR350	271.00	1.06	0.40	75.4	1857	1188	317	51	924
31X-3, 58–60	280.58	SR351	280.58	1.41	0.57	82.3	1883	730	181	32	377
32X-3, 60–62	290.20	SR352	290.20	0.80	0.80	45.5	1867	2385	985	43	871
33X-3, 60–62	299.50	SR353	299.50	1.34	0.75	80.9	1854	962	268	46	BDL
34X-3, 60–62	309.20	SR354	309.20	2.03	1.09	86.7	1765	849	221	48	BDL
35X-3, 57–62	318.87	SR355	318.87	1.39	0.73	65.7	1750	1314	1161	72	BDL
37X-3, 60–62	338.10	SR356	338.10	2.73	–1.40	98.8	826	585	22	26	443

Table T1 (continued).

Core, section, interval (cm)	Depth (mbsf)	Fine iso	Depth (mcd)	Stable isotopes (% VPDB)		$CaCO_3$ (wt%)	Minor elements (ppm)				
				$\delta^{13}C$	$\delta^{18}O$		Sr	Mg	Ba	Fe	Mn
38X-3, 61–63	347.71	SR357	347.71	2.73	–1.33	97.6	798	640	23	34	465
40X-3, 60–62	367.00	SR358	367.00	2.75	–0.94	99.0	779	630	25	46	BDL
198-1209A-											
1H-3, 60–62	3.60	SR181	3.60	0.89	0.80	75.9	1634	1410	125	325	116
2H-3, 60–62	11.80	SR182	11.88	0.51	1.38	57.5	1643	2852	91	555	186
3H-3, 60–62	21.30	SR183	24.36	0.10	0.79	60.0	1605	2317	170	275	203
4H-3, 61–63	30.81	SR184	34.48	0.54	0.74	79.7	1656	1317	83	339	242
5H-3, 60–62	40.30	SR185	44.16	0.63	0.78	89.2	1581	918	39	191	417
6H-3, 60–62	49.80	SR186	54.51	0.45	0.76	88.3	1688	1057	49	273	343
7H-3, 60–62	59.30	SR187	65.31	0.46	0.46	90.2	1630	897	77	330	608
8H-3, 60–62	68.80	SR188	75.39	0.33	0.64	84.1	1604	1150	162	277	733
9H-3, 60–62	78.30	SR189	85.92	0.53	0.78	83.5	1642	954	114	242	626
10H-3, 60–62	87.80	SR190	96.09	0.40	0.22	69.9	1331	2118	683	734	343
11H-3, 60–62	97.30	SR191	107.48	0.95	1.00	77.6	1534	1097	681	306	178
12H-3, 60–62	106.80	SR192	116.16	2.18	1.20	90.7	1500	1283	428	183	61
13H-3, 60–62	116.30	SR195	126.72	1.75	0.20	97.3	1460	583	105	145	8
15H-3, 60–62	135.30	SR196	143.61	1.59	–0.18	97.0	1289	551	163	160	7
16H-3, 60–62	144.09	SR197	153.66	1.83	–0.13	97.8	1084	860	170	116	6
17H-3, 60–62	154.30	SR198	165.54	1.73	0.02	93.9	838	1086	344	199	12
18H-3, 60–62	163.80	SR199	174.78	1.86	–0.15	97.0	623	1341	49	207	7
19H-3, 60–62	173.30	SR200	185.83	1.82	–0.42	96.3	543	1079	71	54	BDL
20H-3, 60–62	182.80	SR201	194.95	0.90	–0.52	98.1	484	1193	38	69	BDL
22H-3, 61–63	201.81	SR202	216.01	3.15	–0.75	98.2	1000	627	12	48	BDL
23H-3, 60–62	211.30	SR203	226.95	3.16	–1.01	96.8	1085	493	127	44	4
24H-3, 60-62	220.80	SR204	235.83	2.40	–0.97	97.1	916	512	116	49	4
26H-3, 60–62	239.80	SR205	256.25	2.92	–0.71	97.4	632	558	9	29	BDL
27X-3, 60–62	249.30	SR206	265.75	2.95	–0.81	98.4	863	638	14	35	BDL
28X-3, 60–62	254.50	SR207	270.95	2.84	–1.18	97.9	840	583	11	BDL	BDL
198-1209C-											
19H-2, 94–96	264.44	SR208	281.07	2.89	–0.96	99.1	755	580	10	25	BDL
20H-3, 60–62	272.00	SR209	288.63	2.72	–1.06	99.4	893	666	9	35	BDL
21H-3, 60–62	281.50	SR210	298.13	2.75	–0.81	97.7	859	616	17	25	BDL
22H-3, 60–62	291.00	SR211	307.63	2.43	–0.73	98.2	888	754	36	37	BDL
198-1210A-											
1H-3, 60–62	3.60	SR212	3.60	0.43	0.44	37.4	1681	2224	418	902	154
2H-3, 60–62	9.50	SR213	11.01	1.54	1.21	82.2	1777	456	44	251	275
3H-3, 60–62	19.00	SR214	20.19	0.04	1.14	65.8	1566	1657	130	184	286
4H-3, 60–62	28.50	SR215	30.78	0.24	0.73	56.8	1407	1574	206	426	211
5H-3, 60–62	38.00	SR216	41.10	0.49	0.98	75.8	1715	653	116	251	512
6H-3, 59–61	47.49	SR217	52.01	0.67	0.93	84.4	1694	505	93	162	471
7H-3, 60–62	57.00	SR218	62.55	0.78	0.94	91.7	1658	369	95	141	578
8H-3, 60–62	66.50	SR219	72.79	0.12	0.36	74.9	1509	1000	235	259	505
9H-3, 60–62	76.00	SR220	83.65	0.39	0.58	87.7	1620	516	120	98	612
10H-3, 60–62	85.50	SR221	93.76	0.24	0.78	62.0	1419	1076	608	187	603
10H-4, 77–79	87.17	SR222	95.43	0.81	1.06	91.4	1412	495	112	82	697
11H-3, 60–62	95.00	SR223	104.56	0.41	0.21	79.8	1250	875	433	238	276
12H-3, 60–62	104.50	SR224	115.84	1.49	1.37	92.8	1368	471	55	74	55
13H-3, 60–62	114.00	SR225	127.00	2.24	1.29	92.9	1270	616	318	103	14
15H-3, 60–62	133.00	SR228	149.71	1.70	–0.15	96.3	1256	346	83	43	BDL
16H-3, 60–62	142.50	SR229	160.36	1.82	–0.07	95.9	907	569	131	127	5
17H-3, 56–58	151.96	SR230	170.61	1.73	–0.18	95.9	675	943	20	75	4
18H-3, 60–62	161.50	SR231	181.03	1.82	–0.44	95.1	597	970	22	67	4
19H-3, 60–62	171.00	SR232	191.89	1.11	–0.35	96.9	481	1156	12	79	5
21H-3, 60–62	190.00	SR233	210.94	3.48	–1.02	96.7	1035	520	4	82	BDL
22H-3, 60–62	199.50	SR234	221.68	3.10	–0.62	97.9	846	566	15	22	21
22H-4, 60–62	201.00	SR235	223.18	3.08	–0.80	98.4	881	434	17	118	5
23H-3, 60–62	209.00	SR236	232.48	2.39	–0.92	97.2	755	685	29	152	4
27H-3, 60–62	239.50	SR238	262.72	2.93	–0.80	98.7	1012	760	15	79	31
198-1210B-											
26H-3, 60–62	240.80	SR239	267.24	2.91	–0.80	96.9	805	633	15	44	41
27H-3, 60–62	250.30	SR240	276.74	3.00	–0.83	97.8	946	630	13	75	120
28H-3, 60–62	259.80	SR241	286.24	2.81	–0.58	97.9	904	801	15	49	132
30H-3, 60–62	273.50	SR242	299.94	2.59	–0.65	98.8	990	699	24	45	49
31H-3, 60–62	282.27	SR243	308.71	2.69	–0.67	96.5	999	687	30	45	74
32H-3, 60–62	292.00	SR244	318.44	2.81	–1.17	97.4	1018	565	27	142	122
33H-3, 62–64	296.52	SR245	322.96	2.68	–1.16	98.2	974	611	70	216	153

Table T1 (continued).

Core, section, interval (cm)	Depth (mbsf)	Fine iso	Depth (mcd)	Stable isotopes (% VPDB) $\delta^{13}C$	$\delta^{18}O$	$CaCO_3$ (wt%)	Minor elements (ppm) Sr	Mg	Ba	Fe	Mn
34H-3, 60–62	304.90	SR246	331.34	2.71	–1.38	98.3	998	591	36	76	78
35H-3, 60–62	313.20	SR247	339.64	2.78	–1.47	98.3	1018	598	43	81	147
36H-3, 60–62	322.20	SR248	348.64	2.63	–1.47	98.6	843	675	25	104	248
37H-3, 60–62	329.80	SR249	356.24	2.66	–1.42	98.1	942	553	28	51	71
38H-3, 60–62	334.80	SR250	361.24	2.64	–1.61	98.6	970	620	28	31	60
41H-3, 60–62	361.60	SR251	388.04	2.76	–1.08	98.5	877	598	26	39	92
42H-3, 60–62	371.10	SR252	397.54	2.70	–1.31	99.6	852	628	28	35	63
198-1211A-											
2H-3, 60–62	6.40	SR253	8.55	0.03	0.87	59.9	1586	1029	136	126	230
3H-3, 59–61	15.89	SR254	18.62	0.36	0.64	80.1	1636	502	25	241	544
4H-3, 60–62	25.40	SR255	28.80	1.08	1.16	78.2	1598	527	31	246	542
5H-3, 60–62	34.90	SR256	39.00	0.25	0.24	75.2	1583	952	250	935	549
6H-3, 60–62	44.40	SR257	49.83	1.04	0.91	90.0	1489	500	14	133	388
7H-3, 60–62	53.75	SR258	60.00	1.79	0.95	98.2	1385	496	22	83	8
8H-3, 60–62	63.40	SR259	69.84	1.85	0.29	85.4	1558	418	109	118	18
9H-3, 60–62	72.90	SR260	80.03	1.88	0.48	97.2	1307	485	10	111	BDL
10H-3, 60–62	82.40	SR261	91.55	2.41	0.46	94.8	1171	427	9	158	5
11H-3, 60–62	91.90	SR262	101.39	1.97	–0.12	92.9	883	691	63	126	5
12H-3, 60–62	101.40	SR263	111.32	1.71	–0.42	94.8	460	1087	19	93	BDL
13H-3, 60–62	110.90	SR264	122.39	1.41	–0.88	95.3	766	811	26	205	6
14H-3, 60–62	120.40	SR265	133.40	3.73	–1.21	98.8	1138	490	9	95	BDL
16H-3, 61–63	139.41	SR268	154.77	2.90	–0.84	98.8	907	674	15	51	BDL
17H-3, 60–62	148.90	SR269	164.26	3.00	–0.82	99.8	925	716	12	50	BDL
18H-3, 60–62	158.40	SR270	173.76	2.88	–0.60	99.6	918	693	17	35	BDL
198-1212A-											
1H-3, 60–62	3.60	SR271	3.75	0.86	2.04	55.1	1750	1387	285	434	175
2H-3, 60–62	8.50	SR272	11.65	0.42	1.18	58.5	1669	1346	200	333	190
3H-3, 60–62	18.00	SR273	21.49	1.16	1.15	75.6	1693	743	115	341	249
4H-3, 60–62	27.50	SR274	30.99	0.55	1.09	83.8	1611	494	129	217	310
5H-3, 60–62	37.00	SR275	40.79	0.48	0.72	88.4	1596	369	84	208	475
6H-3, 60–62	46.50	SR276	50.29	0.15	0.28	88.2	1553	449	108	133	466
7H-3, 60–62	51.00	SR277	58.27	0.00	0.22	73.1	1533	790	172	170	842
8H-3, 60–62	60.50	SR278	68.35	1.70	0.90	85.5	1661	533	511	89	157
9H-3, 60–62	69.82	SR279	79.27	1.25	–0.40	97.3	516	961	23	80	
10H-3, 60–62	79.50	SR280	90.55	3.52	–1.19	98.1	1163	523	6	50	11
11H-3, 60–62	89.00	SR281	100.67	2.71	–0.77	98.2	991	553	16	64	14
12H-3, 60–62	93.50	SR284	103.07	2.91	–0.69	97.7	802	557	13	72	22
198-1212B-											
12H-3, 60–62	105.30	SR285	113.08	3.03	–0.50	97.8	931	746	11	163	183
13H-3, 60–62	114.68	SR286	122.46	2.99	–0.65	97.9	962	686	14	47	23
15H-3, 60–62	125.10	SR287	132.88	2.13	–1.35	94.2	656	632	50	125	22
17H-3, 60–62	140.64	SR288	148.42	2.87	–0.57	98.6	983	627	23	46	21
180-3, 61–63	146.94	SR289	154.72	2.64	–0.56	98.4	996	589	19	57	24
19H-3, 60–62	156.80	SR290	164.58	2.73	–0.81	99.4	926	621	24	73	29
20H-3, 61–63	166.31	SR291	174.09	2.72	–1.00	98.6	992	522	34	108	55
23H-3, 60–62	187.25	SR292	195.03	2.80	–1.08	97.1	924	576	26	48	117

Note: VPDB = Vienna Peedee belemnite.